The Isolated Comet Tail Pseudopodium of *Listeria monocytogenes*: A Tail of Two Actin Filament Populations, Long and Axial and Short and Random

Antonio S. Sechi,* Jürgen Wehland,‡ and J. Victor Small*

*Institute of Molecular Biology, Austrian Academy of Sciences, A-5020 Salzburg, Austria; and ‡GBF, Gesellschaft für Biotechnologische Forschung, Department of Cell Biology and Immunology, D-38124 Braunschweig, Germany

Abstract. *Listeria monocytogenes* is driven through infected host cytoplasm by a comet tail of actin filaments that serves to project the bacterium out of the cell surface, in pseudopodia, to invade neighboring cells. The characteristics of pseudopodia differ according to the infected cell type. In PtK2 cells, they reach a maximum length of ~15 μm and can gyrate actively for several minutes before reentering the same or an adjacent cell. In contrast, the pseudopodia of the macrophage cell line DMBM5 can extend to >100 μm in length, with the bacteria at their tips moving at the same speed as when at the head of comet tails in bulk cytoplasm. We have now isolated the pseudopodia from PtK2 cells and macrophages and determined the organization of actin filaments within them. It is shown that they possess a major component of long actin filaments that are more or less splayed out in the region proximal to the bacterium and form a bundle along the remainder of the tail. This axial component of filaments is traversed by variable numbers of short, randomly arranged filaments whose number decays along the length of the pseudopodium. The tapering of the tail is attributed to a grading in length of the long, axial filaments.

The exit of a comet tail from bulk cytoplasm into a pseudopodium is associated with a reduction in total F-actin, as judged by phalloidin staining, the shedding of α-actinin, and the accumulation of ezrin. We propose that this transition reflects the loss of a major complement of short, random filaments from the comet, and that these filaments are mainly required to maintain the bundled form of the tail when its borders are not restrained by an enveloping pseudopodium membrane. A simple model is put forward to explain the origin of the axial and randomly oriented filaments in the comet tail.

THE intriguing, intracellular propulsion of the pathogenic bacterium *Listeria monocytogenes* has captured the attention of microbiologists and cell biologsts alike (Tilney and Tilney, 1993; Lasa and Cossart, 1996; Pollard, 1995; Southwick and Purich, 1996; Theriot, 1995). Having evolved a method for coercing metazoan cells to collaborate in their self-destruction, these devious parasites as well as others of their kind (Lasa and Cossart, 1996; Theriot, 1995) have inadvertently provided us with a model system to study actin-based motility (Tilney and Tilney, 1993). The movement of *Listeria* inside cells has been likened to that of a comet streaking across the sky (Tilney and Tilney, 1993), since the bacterium moves at the head of a tapering and often curved tail, large enough to be seen in the phase-contrast microscope. We now know that movement itself involves actin polymerization at the bacterium–tail interface (Sanger et al., 1992; Theriot et al., 1992), and that a single bacterial gene product, deposited on the surface of the bacterium, is sufficient to recruit all the components from the host cytoplasm that are required for motility (Domann et al., 1992; Kocks et al., 1992, 1995; Smith et al., 1995; Brundage et al., 1993).

To understand the process of directional locomotion of *Listeria*, we need to characterize the structural organization of actin filaments within the comet tail and define the complexes and control factors responsible for the polymerization and depolymerization of actin filaments within it. Much effort is being expended to achieve the second goal (see, e.g., Pollard, 1995); the present report will concern itself with a reevaluation of the structural organization of the comet tail.

Tilney and colleagues have investigated in depth the organization of listerial comet tails in macrophages, using embedding and thin-sectioning methods for EM (Tilney and Portnoy, 1989; Tilney et al., 1992*a*,*b*). Actin filaments were also decorated in detergent-extracted cells with myosin subfragment 1 to determine filament polarity in the tail.

Please address all correspondence to J. Victor Small, Institute of Molecular Biology, Austrian Academy of Sciences, Billrothstrasse 11, A-5020 Salzburg, Austria. Tel.: (43) 662-63961-11. Fax: (43) 662-63961-40. e-mail: jvsmall@edvz.sbg.ac.at

A.S. Sechi's present address for reprints is Tel.: (49)-531-6181-415. Fax: (49) 531-6181-444. e-mail: ase@gbf-braunschweig.de

Two conclusions of these studies (Tilney et al., 1992*a*) were that actin filaments abutting the bacterial surface do so with their barbed, fast growing ends, and that the filaments constituting the tail are both very short, seldom exceeding 0.2 μm, and randomly arranged. These findings were taken to support a nucleation release model of actin filament dynamics (Theriot et al., 1992), whereby filaments are proposed to be nucleated at the bacterial surface, grow to a limited length, and then become released into the tail, where they are cross-linked into a dense network. Cross-linking is most likely mediated, at least in part by α-actinin, which is abundant in the comet tail (Nanavati et al., 1994). Tilney et al. (1992*a*) also found evidence for a higher concentration of filaments in the lateral margins of the tail and suggested that this hollowlike appearance arises from the contribution of larger numbers of filaments to the tail from the sides of the bacterium than from its rear end. While characterizing the ultrastructure of comet tails, Tilney et al. (1992*a*) noted the marked discrepancy between the tail lengths measured in ultrathin-sections and those obtained by light microscopy. In thin-sections, comet tails were never longer than 3 μm, whereas after phalloidin staining they could be up to 40 μm in length. Therefore, only the proximal region of the tail had been visualized in the embedded material.

Other observations raise additional questions about the deduced length and orientation of actin filaments in the tails. First, Zhukarev et al. (1995) concluded from measurements of fluorescence polarization on phalloidin-labeled comet tails that filaments at the perimeter were preferentially oriented along the long axis of the tail, although conclusions about filament lengths could not be made. Second, in the actin comet tails that propel *rickettsii*, which we may presume form by a mechanism similar or identical to those that trail behind *Listeria*, relatively parallel arrays of actin filaments have been demonstrated in thin-sections (Heinzen et al., 1993).

In light of these observations and especially in view of the susceptibility of nonbundled actin filament arrays to dehydration and embedding procedures (Maupin-Szamier and Pollard, 1978; Small, 1981), we have sought methods to isolate *Listeria* comet tails and analyze their structure using negative staining. To this end, we have managed to isolate the comet tails that protrude from the cell surface as pseudopodia (Tilney and Portnoy, 1989). We have also taken advantage of the finding that, in certain macrophages, protruding *Listeria* continue their motility over extended periods of time and produce pseudopodia of up to ~100 μm in length. The conclusion from these studies is that the comet tail has a core of long axial filaments that is obscured in the proximal region close to the bacterium by a high density of randomly oriented, short filaments. The origin of the two sets of filaments and their relative roles in bacterial propulsion are discussed.

Materials and Methods

Bacterial Stock

The wild-type weakly hemolytic *Listeria monocytogenes* strain EGD (serotype 1/2a) has been described previously (Domann et al., 1992) and was grown in brain heart infusion broth (BHI; Difco Laboratories, Detroit, MI) at 37°C with agitation.

Cell Culture

Hela cells (ATCC-CCL2; American Type Culture Collection, Rockville, MD) were cultured in MEM (Gibco BRL, Vienna, Austria) supplemented with 10% FCS (Sebak, Vienna, Austria), 2 mM L-glutamine, 1% MEM nonessential amino acids, with or without 100 μg/ml penicillin and 100 μg/ml streptomycin (all reagents purchased from Gibco BRL); Ptk2 cells (ATCC, CCL 56) were routinely cultured in the Hela cell medium given above, supplemented with 1 mM sodium pyruvate (Gibco BRL). The mouse macrophage cell line DMBM5, kindly provided by Dr. D. Monner (GBF, Braunschweig, Germany), was grown in DME supplemented with 10% horse serum, 5% FCS, 10% L cell conditioned medium (LCM), 2 mM L-glutamine, 1% nonessential amino acids, 200 μg/ml biotin, and 100 μg/ml vitamin B12 (Sigma, Vienna, Austria) without antibiotics. LCM was obtained as the medium produced by mouse L929 fibroblasts after 4 d of growth at confluency in DME supplemented with 10% FCS and 2 mM L-glutamine in the absence of antibiotics, and was filtered before use. All cell lines were grown at 37°C in the presence of 7% CO_2.

Infection

The cultured cell lines were plated into 3.5-cm petri dishes (Falcon Laevosan, Linz, Austria) 1 d before the experiment and used at 60–70% confluency. For light microscopy, cells were plated onto 24 × 24-mm coverslips in the same dishes. Bacteria were grown to an optical density of 1.4–1.5 at 600 nm, corresponding to around 10^9–10^{10} colony forming units (CFU) per ml.

To infect the cells, bacteria were washed twice in PBS; after the final wash, the pellet was resuspended in infection medium (standard cell medium lacking antibiotics and serum) to give a final bacterial concentration of 10^6–10^7 CFU/ml. Cells were washed three times with prewarmed (37°C) infection medium. To enhance and synchronize the infection process, 1 ml of the bacterial suspension was added to each 3.5-cm dish, and the dishes were centrifuged at 700 *g* for 5 min at room temperature. Cells were then returned to the incubator for 1 h to permit bacterial entry. Subsequently, cells were washed three times with standard medium containing serum, but lacking antibiotics; after the final wash, 15 μg/ml of gentamicin was added and the cells were returned to the incubator for at least 5 h (the optimal time depending on the cell line used).

Isolation of Pseudopodia

Infected cells were washed three times in cytoskeleton buffer (CB: 10 mM MES, 150 mM NaCl, 5 mM EGTA, 5 mM $MgCl_2$, 5 mM glucose, pH 6.1). After the last wash, 1 ml of fresh CB was added to the dish. Using a 1-ml automatic pipette, the cells were then repeatedly and gently flushed with the buffer to detach the pseudopodia. These were then centrifuged onto copper electron microscope grids, sandwiched between a Formvar film and a glass coverslip (see Small and Herzog, 1994) in a fresh petri dish, at 2,000 *g* for 5 min at room temperature. Sedimented pseudopodia were then washed with CB and processed for EM.

More complete details of the isolation procedure have been presented elsewhere (Sechi and Small, 1997).

EM and Subfragment 1 Labeling

Sedimented pseudopodia, on the coverslip–grid supports, were extracted in a mixture of 0.5% Triton X-100, 0.25% glutaraldehyde in CB for 60 s, and then fixed with 2.5% glutaraldehyde in CB for 10 min. They were rinsed three times in CB, and the actin filaments were stabilized by incubation in 10 μg/ml phalloidin (a gift from Prof. H. Faulstich, Heidelberg, Germany) in the same buffer (see Small and Herzog, 1994) for at least 20 min or until use. The grids were removed from the coverslips, negatively stained with aqueous 3% sodium silico-tungstate, and observed in an EM10A electron microscope (Zeiss, Oberkochen, Germany) operating at 80 kV.

For labeling with myosin subfragment 1 (S-1)[1] isolated pseudopodia on grids were extracted with 0.5% Triton X-100 in CB for 60 s, and then incubated with smooth muscle myosin S-1 (kindly supplied by Dr. A. Sobieszek, Salzburg, Austria) at a concentration of 0.5 mg/ml in S-1 buffer (0.1 M KCl, 10 mM Tris-HCl, pH 7.0) for an additional 60 s. The grids were rinsed three times in S-1 buffer, and then fixed in 2.5% glutaralde-

1. *Abbreviation used in this paper*: S-1, subfragment 1.

hyde in CB for 10 min. They were subsequently rinsed in CB and negatively stained as above.

Immunofluorescence Microscopy

Infected cells were fixed in one of two ways. For α-actinin labeling, we used a mixture of 3% paraformaldehyde, 0.3% Triton X-100, 0.1% glutaraldehyde in CB for 15 min. For ezrin labeling, infected cells were fixed with 0.5% paraformaldehyde in CB for 15 min, and then extracted with 0.2% Triton X-100 in CB for 15 min. Primary antibodies were: a monoclonal α-actinin antibody from Sigma (BM-75.2), and a polyclonal ezrin antibody raised against human ezrin (kindly supplied by Dr. A. Bretscher, Cornell University, Ithaca, NY) that does not cross-react with moesin or radixin (Franck et al., 1993). Fluorescent labeling (for general conditions see Herzog et al., 1994) was achieved using either a two-step procedure (α-actinin) using Cy3-conjugated goat anti–mouse IgM (62-6815; Zymed Laboratories, S. San Francisco, CA) or a three-step procedure (ezrin) using biotinylated goat anti–mouse IgG (E433; DAKO, Glostrup, Denmark) followed by Cy2-conjugated streptavidin (Biological Detection Systems, Inc., Pittsburgh, PA). Double labeling for actin was carried out by adding fluorescein or rhodamine-conjugated phalloidin (a gift from Prof. H. Faulstich, Max Planck Institute, Heidelberg, Germany) in the final incubation step. Coverslips were mounted in Gelvatol containing 2.5 mg/ml *n*-propyl gallate as antibleach agent, and images were recorded on a Zeiss Axiovert 135 TV inverted microscope equipped with a cooled and back-illuminated CCD camera (Princeton Instruments, Inc., Princeton, NJ), controlled by IP-Labs software.

Video Microscopy

For video microscopy, coverslips carrying infected cells were attached with grease to petri dishes bearing a 15-mm-diam hole in their base (McKenna and Wang, 1989), and the cells were maintained in L15 medium on a homemade heating stage mounted on the inverted microscope. The cells were observed in phase contrast or differential interference contrast using a ×40 (NA 0.66) Achroplan LD objective. Sequences were recorded in real time on videotape using a C2400-77 camera with an Argus 10 controller (Hamamatsu Photonics, Herrsching, Germany) and converted into time-lapse series as described by Anderson et al. (1996).

Results

Characteristics of Comet Tails in Pseudopodia

In initial attempts to determine actin filament organization in comet tails, we prepared whole mount cytoskeleton of *Listeria*-infected cells using methods described previously for monolayer cultures (Small and Herzog, 1994). By this means, intracellular comet tails could be identified, but the superimposition of the host cell cytoskeleton made it difficult to unambiguously define the structure of the tails. We therefore sought methods to isolate the tails from infected cells. This was practically feasible in later stages of infection when many bacteria emerge from the cell surface in the pseudopodia formed as a prelude to the invasion of other cells. Since our structural data focus on the pseudopodia, it was necessary to consider any differences in their motility, form, or composition as compared with the comet tails in the bulk cytoplasm. Some motile characteristics of pseudopodia formed by *Listeria* have also been documented by Sanger et al. (1992).

Fig. 1 *a* shows a video series of an infected PtK2 cell in which the fate of two comet tails can be followed. The first (Fig. 1 *a*, *1*) already existed as a pseudopodium for 3 min before the beginning of the sequence and actively waved around in the medium for an additional 4 min before reentering the parent cell and immediately continuing its movement. The second (Fig. 1 *a*, *2*), started in the main body of the cell, formed a pseudopodium, and then reinvaded the cell within the sequence, spending only 2 min as a pseudopodium. For this latter type of protrusion, the velocity of movement of the bacterium in the protruding phase was the same as in the bulk cytoplasm. Measurements showed the average lifetime of pseudopodia to be ~3 min ± 1 min (15 measurements), and the rate of movement inside growing pseudopodia averaged 0.074 μm/s (SD ± 0.01 μm/s) as compared with a rate of 0.15 μm/s (SD ± 0.04 μm/s) for bacteria freely moving in the cytoplasm.

For the macrophage cell line, the *Listeria*-induced pseudopodia exhibited a markedly different behavior (Fig. 1 *b*). In contrast with those formed in PtK2 cells, the macrophage pseudopodia could extend far away from the parent cell for up to 100 μm or more (measured maximum, 127 μm). The velocity of bacteria at their tips (0.094 ± 0.046 μm/s) was equal to that of bacteria driven by comets in the main body of the cell (0.100 ± 0.045 μm/s). For Hela cells, the pseudopodia were of limited length (~30 μm) but were often longer than those found on PtK2 cells (~15 μm).

After phalloidin labeling, it was evident that there was a lower amount of F-actin in the pseudopodia, as compared with the tails in the cell body. The tails in the pseudopodia appeared generally slimmer and, for the longer ones, the phalloidin label tapered down to a thin stalk that connected to the cell periphery (Fig. 2, *a–d*). This difference in morphology between comet tails in the deeper cytoplasmic and pseudopod compartments correlated with the changes in phase density observed in the phase-contrast microscope. In the bulk cytoplasm, the tails appeared diffuse, whereas in the pseudopods, where they were delimited by the cell membrane, they appeared more phase dense and compact.

The most significant difference between tails in the pseudopodia and those elsewhere was with respect to the localization of α-actinin. Comet tails in the main body of the cells were strongly labeled for α-actinin whereas those in the pseudopodia were unstained (Fig. 2, *e* and *f*). The shedding of α-actinin from the tails as they entered pseudopodia was clearly evident for those tails that still had their trailing parts within the main cell boundary (Fig. 2, *g* and *h*). Another feature specific for the pseudopodia was the presence of ezrin on the membrane that enveloped them (Fig. 2, *i* and *j*). Both the absence of α-actinin and the presence of ezrin in the pseudopodia served to distinguish them clearly from the comet tails in the main cell body.

Isolation and Structure of Pseudopodia

The isolation of *Listeria*-induced pseudopodia in sufficient yield was greatly facilitated by the high level of infection of cells (~100%) achieved by centrifuging the bacteria onto the cell monolayers. As isolated, the pseudopodia still retained a membrane envelope and were sedimented in this state onto the plastic support films used for EM. Visualization of the comet tail cytoskeletons involved the same fixation–extraction procedures found suitable for revealing actin filament meshworks in cultured cell lamellipodia (Small, 1981). This included a postfixation treatment with phalloidin to stabilize the actin filaments.

In line with the differences noted in the light microscope, pseudopodia isolated from PtK2 cells showed subtle differences in structure to those from the macrophage cell line. First of all, they differed in length, the isolated

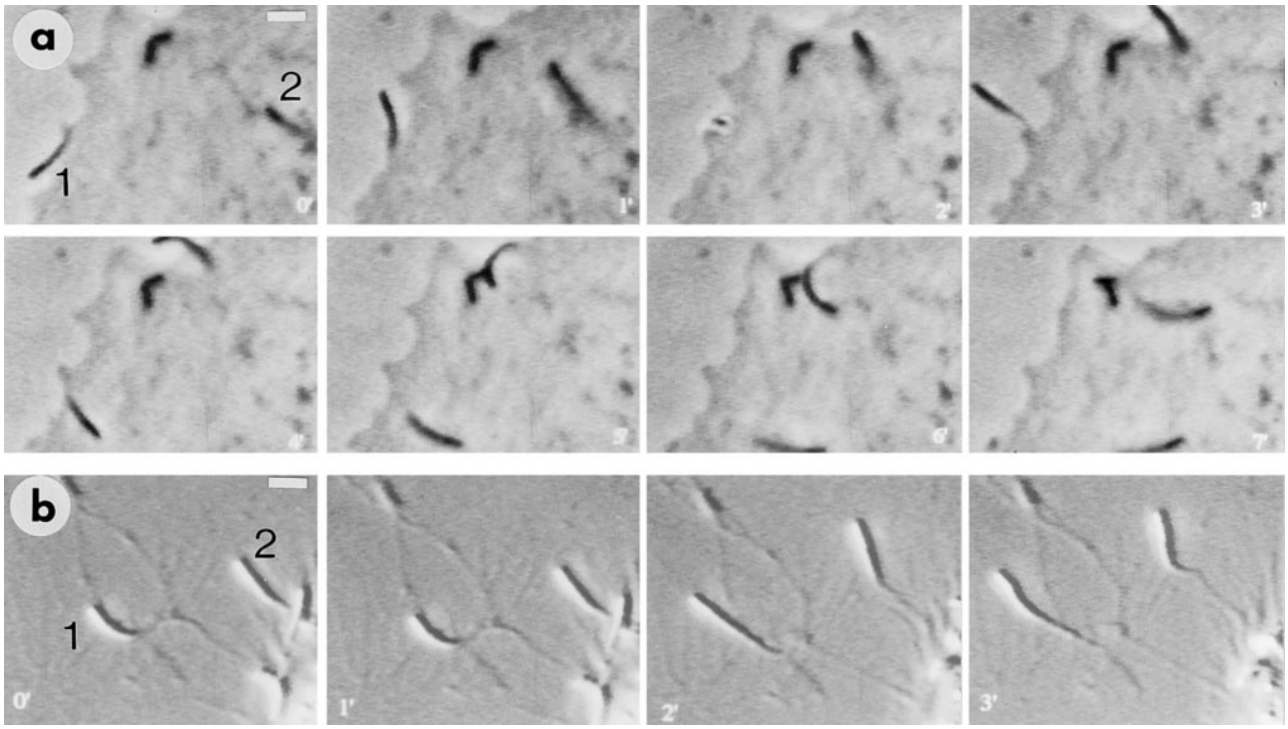

Figure 1. Video sequences showing *Listeria*-induced pseudopodium behavior in PtK2 cells (*a*) and macrophages (*b*). Time is indicated in min. (*a*) One bacterium is already in a pseudopodium (*1*) at time 0′, and the second (*2*) is in bulk cytoplasm at the head of a comet tail. The pseudopodium (*1*) gyrates actively for several minutes, and then reenters the main body of the cell at around 5′, forming a typical comet tail (*6′* and *7′*). The second bacterium begins to form a pseudopodium at 2′, which then exists from 3′ to 5′, after which the bacterium reenters the cell (at *6′*), immediately forming a comet (*7′*). (*b*) Two pseudopodia (*1* and *2*) are shown that have already extended away from the macrophage cell body (*bottom righthand corner*) and continue to move during the sequence, being tethered to the cell by a thin strand. Conditions: (*a*) phase contrast; (*b*) Normarski interference contrast. Bars: (*a* and *b*) 4.5 μm.

PtK2 pseudopodia averaging 7 ± 2.4 μm and those from macrophages 16.5 ± 4.7 μm. But most notably, PtK2 pseudopodia characteristically exhibited more randomly organized short filaments throughout their length, especially in the region proximal to the bacterium (Fig. 3). Measurements showed the random filaments to fall in the length range of 0.3–1.0 μm, with a mean of 0.57 ± 0.17 μm. In addition to these randomly oriented filaments, a set of long filaments aligned along the axis of the tail was also evident. These filaments were somewhat dispersed in the proximity of the bacterium and became progressively bundled towards the midpart and end of the tail. Fig. 4 shows a thin PtK2 pseudopod that spread out laterally on the support film, revealing rather clearly the two sets of actin filaments, random and longitudinal. In this example the continuity of the longitudinally arranged filaments is especially evident and can be emphasized by tilting the micrograph to view the filaments at a grazing angle. Single filaments could be traced for up to 2 μm along their length, before being lost in the more densely packed regions.

Fig. 5 shows a typical macrophage pseudopodium. The most striking feature is the clear presence of a bundle of axially oriented filaments that splays out into single filaments towards the rear of the bacterium. Short, randomly oriented filaments are also present, but they are far less abundant than in the PtK2 pseudopodium. The tapered end of the tail shows exclusively parallel actin filaments, and there is no indication of multiple discontinuities within the filament bundles, as would be expected for assemblies of short, interconnected filaments. Fractures in the tail bundles, with the appearance of free filament ends, however, were observed in regions of sharp curvature (not shown). We presume that these fractures arose during the sedimentation of the tails onto the support film, or during the pipetting step. An additional example of a macrophage pseudopodium (Fig. 6) clearly shows a parallel array of long actin filaments as the dominating feature of the comet tail.

Filament Polarity

To gain information about filament polarity, we also labeled isolated and Triton-extracted pseudopodia with myosin S-1, before fixation and negative staining. Since the labeling density was so high, it was difficult to ascertain arrowhead directions in the bulk of the tail. However, at the end of the tail, almost all filaments were oriented with their pointed ends towards the tip (Fig. 7). Interestingly, S-1 decoration commonly dislodged the bacterium from the head of the tail and revealed filaments, with few exceptions, showing barbed ends, in agreement with the data of Tilney et al. (1992*a*). Thus, we could confirm that the fast growing ends of the actin filaments abut the bacterium.

Discussion

Tilney and Tilney (1993) note that the primary function of

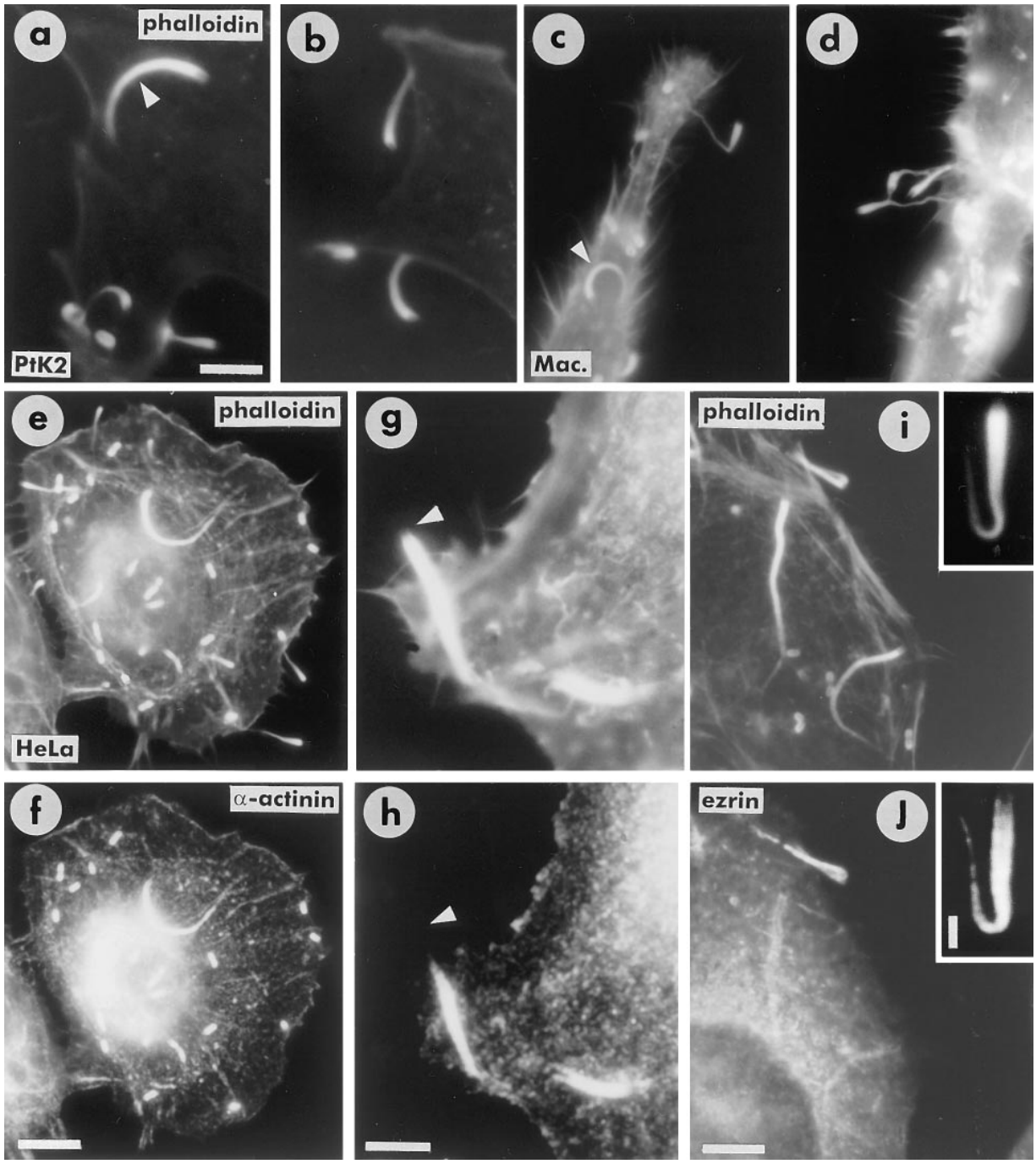

Figure 2. Characteristics of pseudopodia from PtK2 cells (*a* and *b*), macrophages (*c* and *d*), and Hela cells (*e* and *f*). (*a–d*) Difference in appearance between *Listeria* comet tails (*arrowheads* in *a* and *c*) and pseudopodia (*a–d*) after phalloidin staining. (*e* and *f*) Presence of α-actinin in comet tails and absence from pseudopodia. Pseudopodia are clearly identified by phalloidin label (*e*) but are negative for α-actinin (*f*). (*g* and *h*) A comet tail in the process of forming a pseudopodium and showing the lack of α-actinin in the protruding region. Arrowheads indicate position of rear end of bacterium. (*i* and *j*) Ezrin is present in pseudopodia but not in comet tails in the main cell body (the faint label of the tails in the cell body in *f* is due to some bleedthrough from the rhodamine channel (*i*). (*Inset*) Labeling of a pseudopodium that had detached from a cell but was still bound to the coverslip. Bars: (*a–d*, *i*, and *j*) 7.5 μm; (*e* and *f*) 12 μm; (*g* and *h*) 5 μm; (*inset*) 1.8 μm.

the *Listeria* comet tail is to form a pseudopodium, as a prerequisite for the dissemination of infection. In this study we have isolated the pseudopodia and demonstrated the organization of actin filaments within them. We show that there are two populations of actin filaments: a more or less parallel array of long, axial filaments that appear graded in length, and a set of randomly oriented short filaments that progressively decrease in abundance from the head towards the tip of the tail. Before discussing the implications of this organization of actin, it is worth considering why the longitudinal component of filaments has been missed in earlier studies.

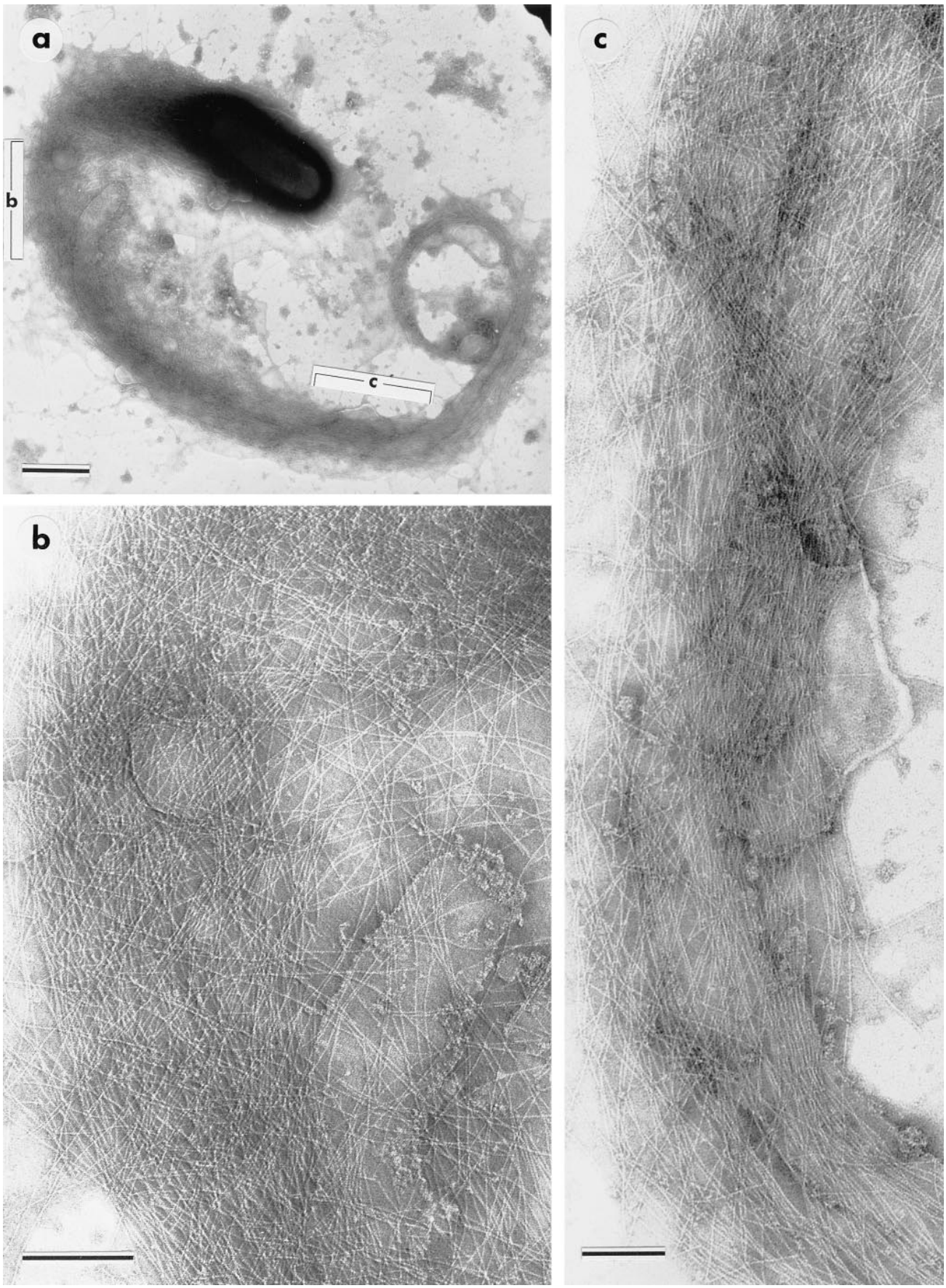

Figure 3. Isolated PtK2 pseudopodium (*a*) indicating regions (*bracketed*) shown at higher magnification in *b* and *c*. The component of axial filaments in *b* is best revealed by viewing the micrograph at a glancing angle. Bars: (*a*) 1 μm; (*b* and *c*) 0.2 μm.

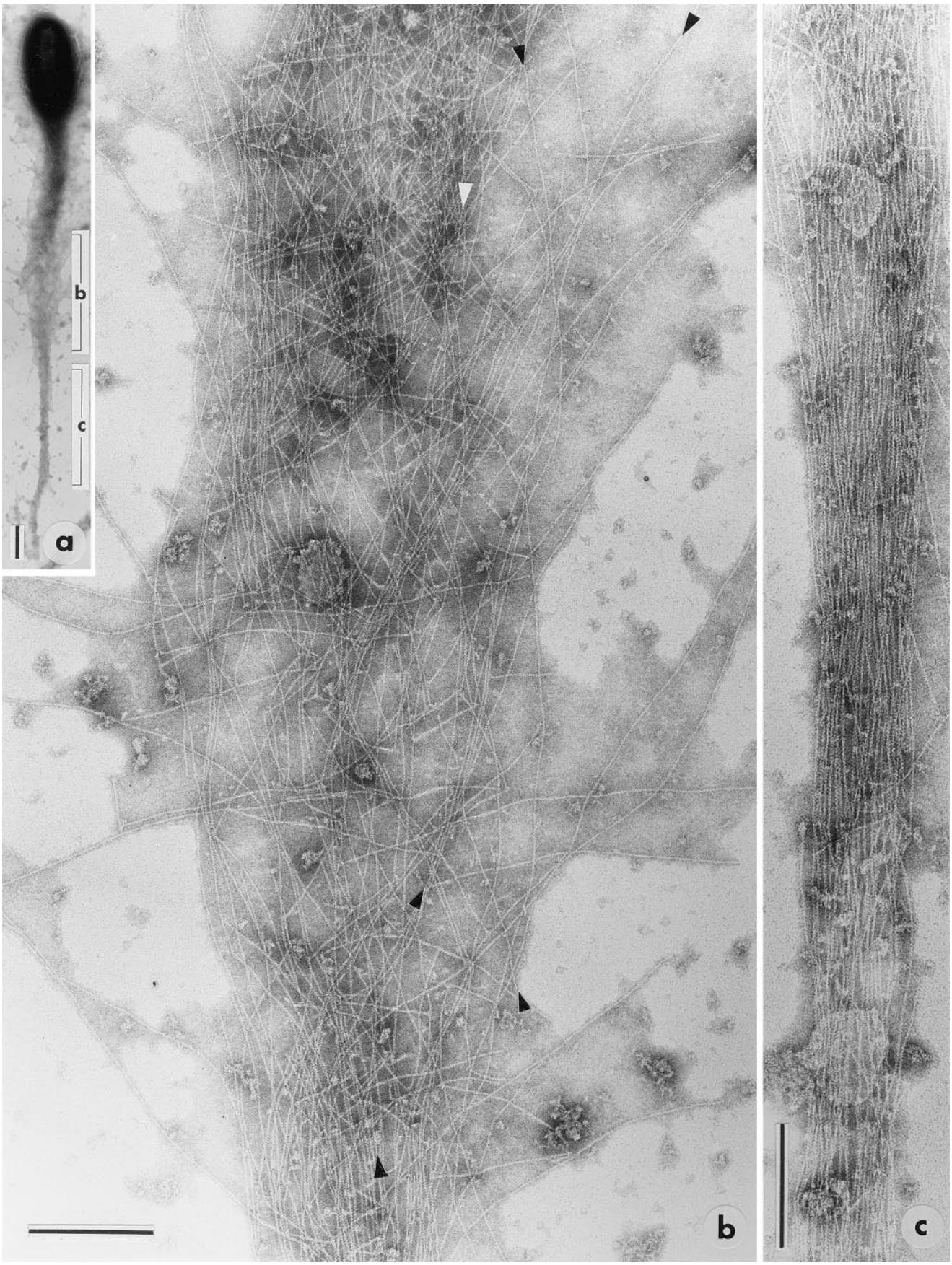

Figure 4. Isolated PtK2 pseudopodium (*a*) that was well spread in the medial part of the tail. Electron micrographs in *b* and *c* show enlargements of the corresponding regions indicated in *a.* In *b* the continuity of the axial filaments is particularly evident, when the micrograph is viewed at a grazing angle. The filaments marked with arrowheads, as well as others, can be followed through most of the micrograph. Bars: (*a*) 1 μm; (*b* and *c*) 0.2 μm.

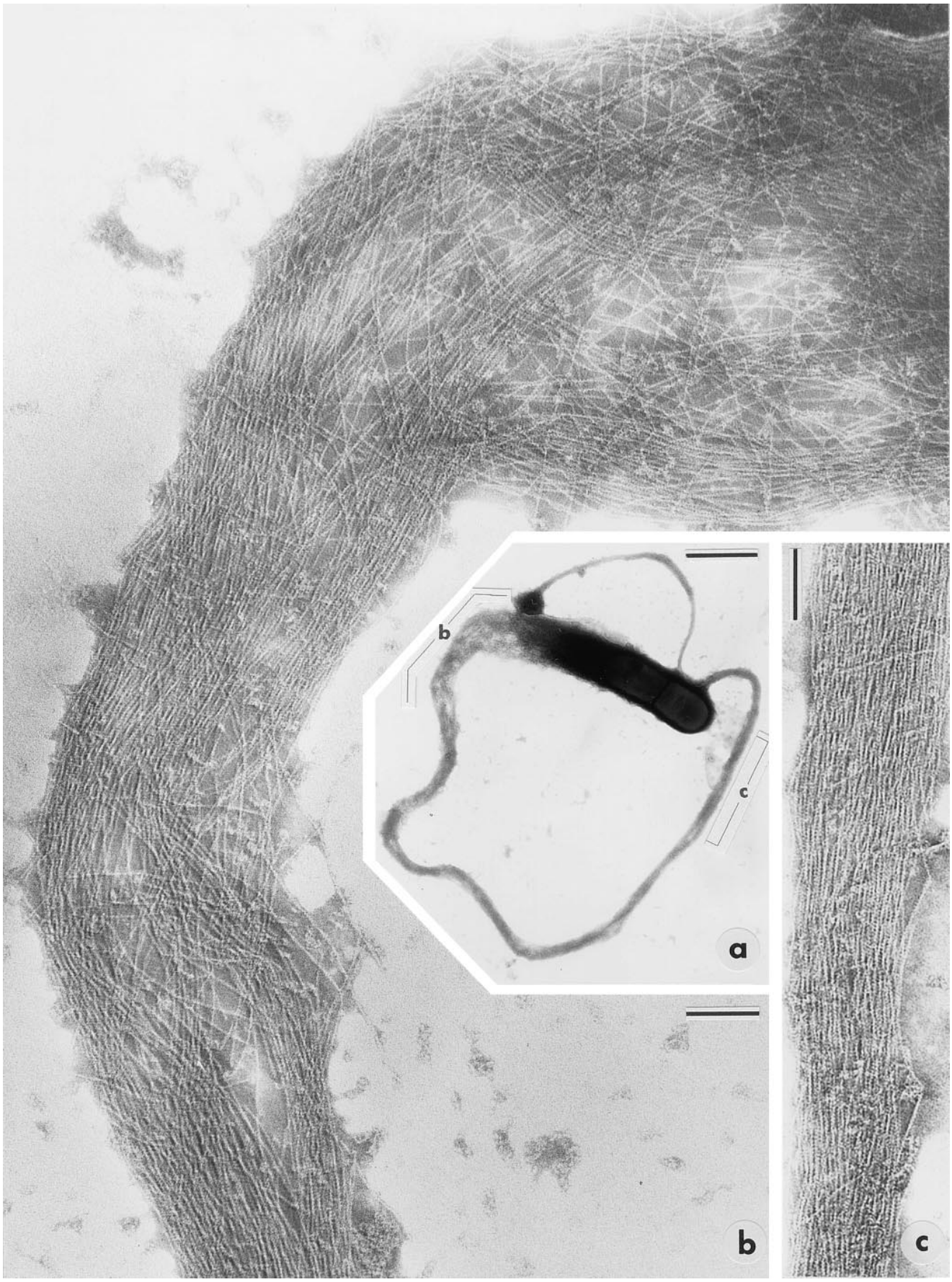

Figure 5. Isolated macrophage pseudopodium (*a*) indicating regions (*bracketed*) shown at higher magnification in *b* and *c*. Note splaying of long, axial filaments into the region proximal to the rear of the bacterium (*top right* in *b*). Bars: (*a*) 1 μm; (*b* and *c*) 0.1 μm.

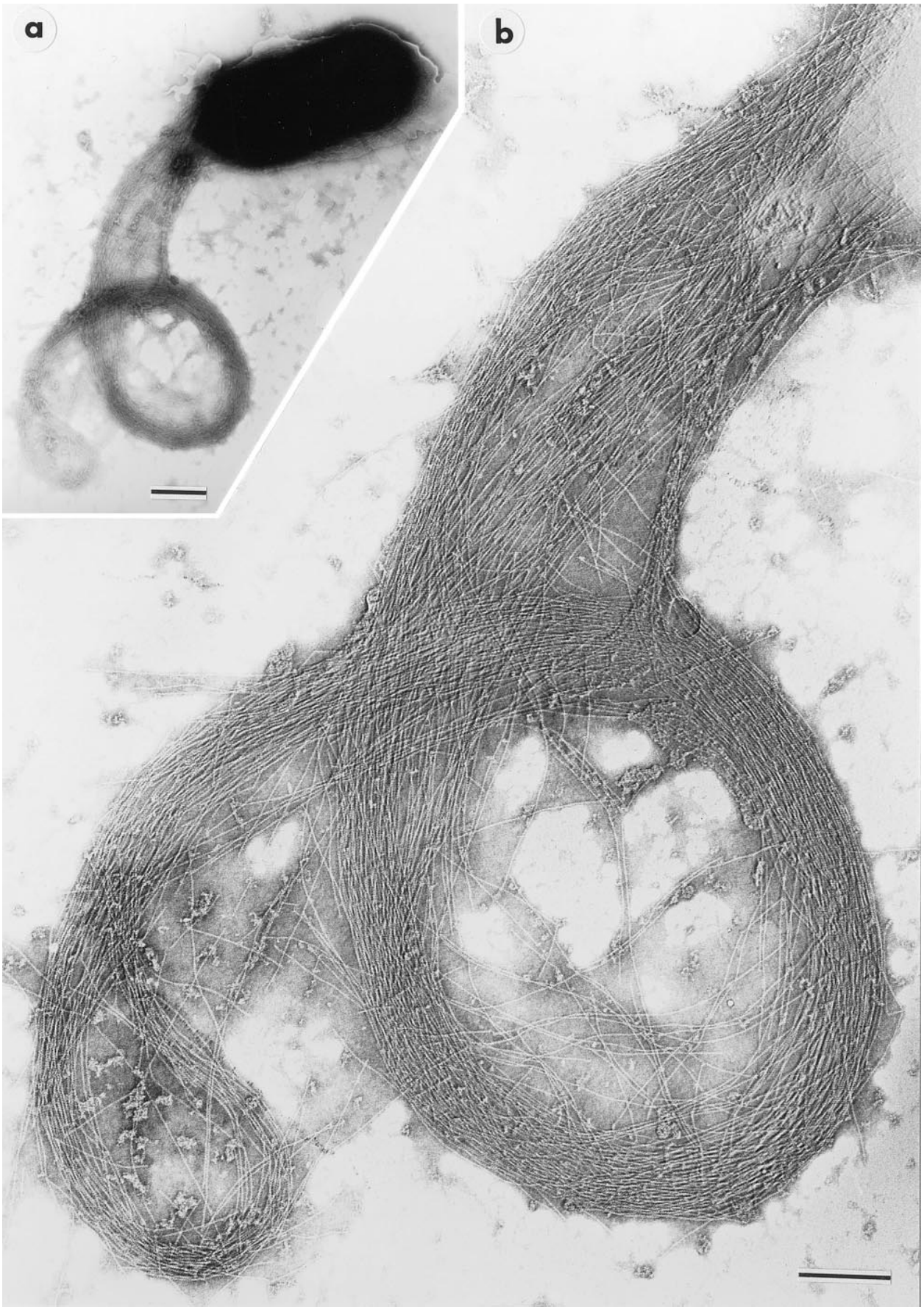

Figure 6. Isolated macrophage pseudopodium (*a*), at higher magnification in *b*, that shows a prominent axial array of long actin filaments. Bars: (*a*) 0.5 μm; (*b*) 0.2 μm.

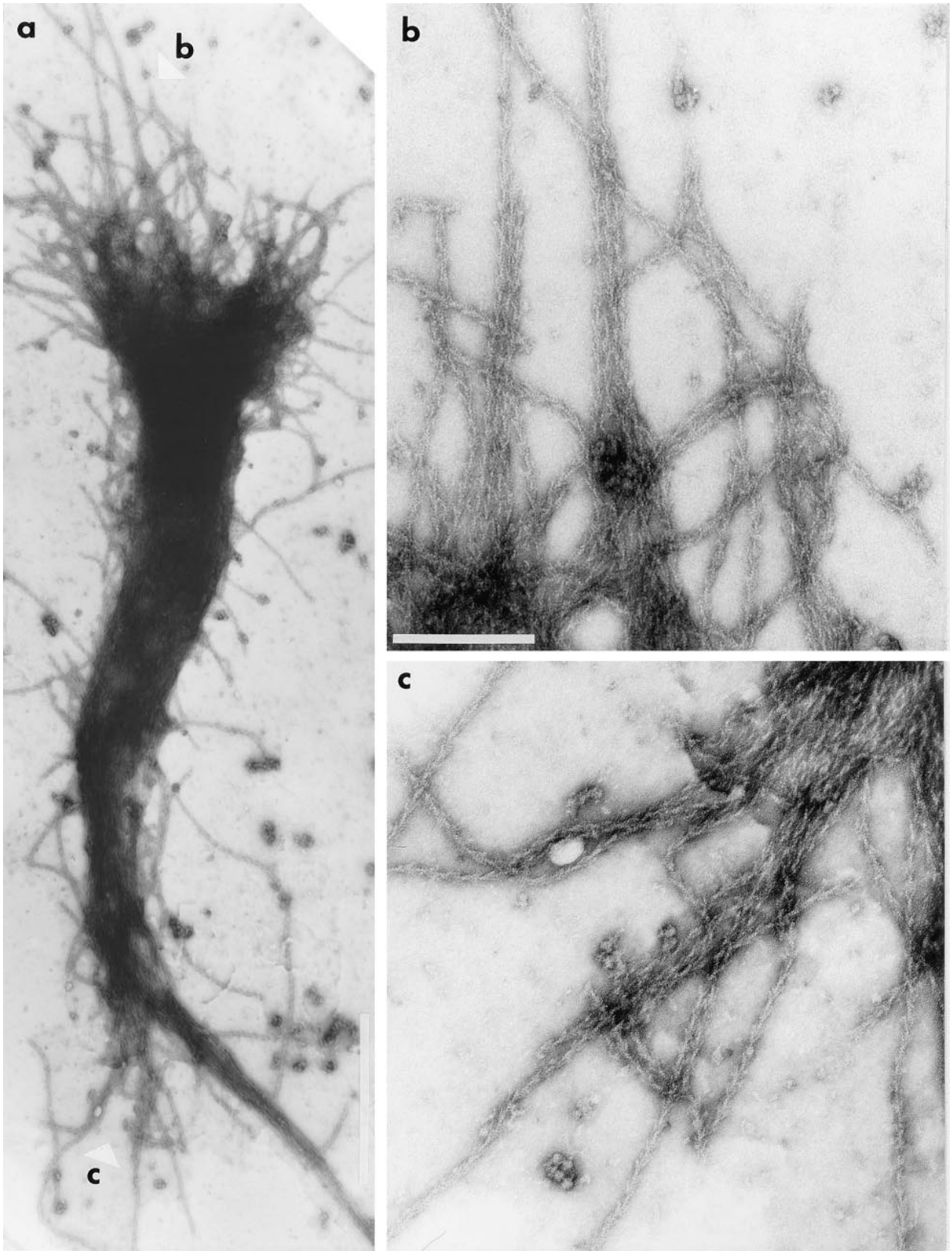

Figure 7. Isolated pseudopodium (*a*, overview) labeled with smooth muscle myosin S-1 and showing, in *b* and *c*, the actin filament polarity at the two ends: (*b*) head end and (*c*) trailing end. The positions of the regions enlarged in *b* and *c* are indicated in *a* (*white arrowheads*). The loss of bacterium from the head end is a typical consequence of S-1 labeling. Bars: (*a*) 1 μm; (*b* and *c*) 0.2 μm.

Relatively open networks or arrays of actin filaments, as occur, for example, in lamellipodia, are notoriously difficult to visualize in plastic embedded material. Since the problem escapes most contemporary authors, it is necessary to reemphasize that this arises from the adverse effects that both osmium tetroxide and dehydration in organic solvents have on the integrity of F-actin (Maupin-Szamier and Pollard, 1978; Small, 1981, 1985, 1988). Complexing actin with myosin head subfragments confers some stability during the cited processing steps and provides a convenient polarity marker, as was first shown for nonmuscle cells by Ishikawa et al. (1969). This explains why published images of embedded *Listeria* comets have invariably revealed a fuzzy, nondescript structure except when the filaments were decorated with myosin heads (Tilney and Portnoy, 1989; Tilney et al., 1992*b*). Only then could discrete filaments be identified. Nevertheless, the task of tracing filaments was still compromised by the limitations set by section thickness, as well as by any subtle reorganizations induced by the decoration of the detergent-extracted tails with myosin heads. As already noted (see Introduction), Tilney et al. (1992*a*,*b*) were aware of having captured only the first few microns of the comet tails in sections, probably because of the invariably curved form of the comets. It is in this proximal region that the axial filaments are more dispersed than in the distal parts of the tail, since here they splay out into the rear of the bacterium. We conclude that this regional splaying of the axial filaments explains why they have been overlooked in thin-sections of myosin-stabilized preparations (Tilney et al., 1992*b*).

Inasmuch as the pseudopodia are motile and can revert rapidly into their parent comet tails on reentry into bulk cytoplasm (e.g., Fig. 1 *a*), we can presume that the basic mechanism of movement of *Listeria* in the main body of the cell and in the pseudopodia is identical. Changes do, however, occur as the comet tails enter the protrusion phase; α-actinin is lost and there is a decrease in total F-actin, as judged by the intensity of phalloidin staining. We propose that the decrease in actin cross-linking that presumably results from the loss of α-actinin leads to the shedding of a sizeable proportion of the short filaments from the comet tail as it forms a pseudopodium. Dold et al. (1994) have indeed shown that the comet tails are disrupted in cells microinjected with a gelation-incompetent fragment of α-actinin, suggesting that this protein here plays a major role in filament cross-linking. A reduction of cross-linking would at the same time facilitate a collimation of the longitudinal filaments into a more compact bundle, as seen in the isolated pseudopodia. In this context, the short filaments are seen as structural elements required for long distance, lateral cross-linking within the comet tail (Fig. 8 *a*) and between the tail and the surrounding cytoskeleton. In the realm of bulk cytoplasm, such a function is vital to restrain the borders of the tail and to give it polarity and support, but it becomes of lesser importance in the membrane-coated pseudopodia. Dabiri et al. (1990) have previously claimed that α-actinin is present in pseudopodia, but inspection of their images reveals that the intensity of fluorescent label in pseudopodia was the same as in the nonspecific background in the cell.

It has been shown that the actin comet tail induced by

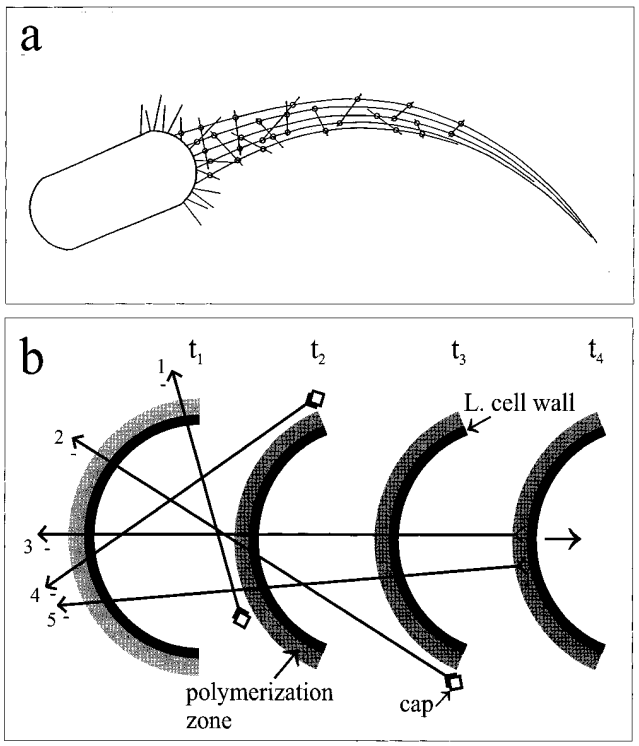

Figure 8. (*a*) General organization of actin filaments in pseudopodia. Long filaments provide the axis of the tail, and short filaments cross-link them (*circles*) into a loose bundle in the region proximal to the bacterium. The comet tails are presumed to have the same structure as the pseudopodia, except that they feature more randomly arranged short filaments. In the more distal parts of the tail, where there are fewer short filaments, the cross-linking between axial filaments predominates (not indicated). (*b*) Schematic illustration of how the short and long filaments may be generated. The rear end of the bacterium is depicted at different stages of forward movement (*arrow*) at times t_1–t_4. The grey, external layer houses components of the polymerization machinery that nucleates actin filaments and feeds their barbed (+) ends with actin monomers. When a filament (+) end lies outside this polymerization zone, it is capped by host cell capping factors (*squares*). For clarity, only a few actin filaments (*straight lines*) are shown. Arrowhead configurations indicate the pointed (−) and barbed (+) ends of the filaments. The lengths of a filament will be determined by the position on the rear of the bacterium at which it becomes nucleated and the orientation to the membrane adopted at that time (we assume this to be variable), since this will define how long the filament can reside in the polymerization zone as the bacterium moves forward. The ends of filaments 1 and 4 fall out of the influence of the polymerization zone at t_2, after they become tangential to its outer surface. They will be short and obliquely oriented to the tail axis. For filament 2, polymerization ceases at t_3. By the same token, more axially oriented filaments (*3* and *5*) will maintain their plus ends in the polymerization zone for a more extended period and thus become correspondingly longer. *L. cell wall*, *Listeria* cell wall.

Listeria is itself immobilized in the cytoplasm (Sanger et al., 1992; Theriot et al., 1992), and that forward propulsion of the bacterium results from the polymerization of actin at the membrane surface of its trailing end (Sanger et al., 1992; Theriot et al., 1992; Tilney et al., 1992*b*). Specific and exclusive insertion of actin monomers at the head of the tail

has also been shown for the related comets that form behind vaccinia virus in infected host cytoplasm (Cudmore et al., 1996). Since only very short (0.2 μm) filaments could be identified in *Listeria* comets in thin-sections (see references cited above) and the tails were many microns long, it was proposed that a "nucleation-release mechanism" (Theriot and Mitchison, 1991) could best explain the actin filament dynamics in the tail (Theriot et al., 1992). Measurements of actin filament half-life in the tails were also taken to support this mechanism (Theriot et al., 1992). In the nucleation-release model, actin filaments are associated with the bacterium surface for only as long as it takes them to reach a length of ~0.2 μm and to become cross-linked into the preexisting tail. They are then released by the bacterium so that new actin filaments can be nucleated in their place. Our new data on pseudopod structure are inconsistent with this model and indicate that another mechanism is at play.

The scheme we suggest is depicted in Fig. 8 *b.* As in other schemes, actin filaments are nucleated at the bacterial surface with their fast growing barbed ends abutting this interface (Tilney et al., 1992*b*). Nucleation and polymerization is presumably effected by complexes containing ActA and other components (e.g., Pollard, 1995) residing in a layer coating the outside of the bacterial membrane. We presume that the growing filament end can move over the membrane surface, recruiting monomers from this zone of actin polymerization. Two further assumptions are made: (*a*) that the actin filaments remain closely linear; and (*b*) that they cease to polymerize soon after their orientation becomes tangential to the polymerization zone (Fig. 8 *b*), after which point they fall out of its influence. On the basis of these assumptions, it is readily possible to explain the presence of long axial filaments and short random filaments in the comet tails according to the location on the rear surface of the bacterium and the orientation at which they were nucleated. (If the angle of orientation to the membrane is fixed, e.g., at 90°, only the site of nucleation will determine the filament length, but the consequence is essentially the same.) Filaments 1 and 4 in Fig. 8 *b* become tangential to the polymerization zone and fall away from it at time t_2. They are then capped and contribute short, oblique filaments to the tail. The existence of capping factors that block polymerization of all comet tail filaments not associated with the rear end of the bacterium is indicated by previous findings (Tilney et al., 1992*b*; Sanger et al., 1992). Other filaments that are nucleated with an axial orientation (Fig. 8 *b*, *3* and *5*), maintain their plus ends in the polymerization zone for an extended time and grow correspondingly longer.

Mogilner and Oster (1996) have put forward an interesting model to explain actin-based *Listeria* motility and lamellipodium protrusion. They propose that the actin filaments undergo thermal bending motions large enough for the plus ends to move away from the membrane for monomer insertion and thus for polymerization to occur. In this scheme, the lengthening filaments push against the rear of the bacterium by "vibrating" against it. We only note that the force exerted by a filament, for this model, is predicted to be greater for obliquely oriented filaments than for axial filaments (Oster, G., personal communication). Whether or not actin monomer insertion for an actively pushing filament requires thermal fluctuations of the filament or another mechanism, e.g., one that uses a motor molecule incorporated into the membrane-associated polymerization complex, remains to be established.

The presence of long axial filaments and short, more transverse filaments readily explains the cometlike form of the tail. The long filaments provide an axial component that is bound into a compact tail by cross-linking with the short filaments. In more distal parts of the tail, where the number of short filaments is diminished, owing to their short half-life (Theriot et al., 1992), cross-linking between the long filaments themselves presumably predominates. As we have shown, the number of short filaments seen in the isolated *Listeria* pseudopodia depended on the infected cell type, many more being seen in PtK2 pseudopodia than in those from macrophages. While this could be explained by the longer lifetime of the macrophage protrusions, there may be real variability in tail structure. It is notable in this respect that the comet tails formed behind *Shigella* appear thinner than those from *Listeria* (Zeile et al., 1996). We suggest that this may be explained by a tail composed mainly of axial filaments and relatively few short filaments. At the other extreme are tails formed behind vaccinia virus, which appear to contain a large complement of short filaments (Cudmore et al., 1996). While the reasons for these differences are not presently clear, they may arise from differences in pathogenic factors and from variations between cells in factors that control actin filament dynamics, as well as from differences in the geometry of the transported particle. Using the techniques developed here, the structure–function relationships underlying these differences may now be more amenable to investigation. We may also expect that the availability of isolated pseudopodia will help hasten the quest to identify the accessory components required for actin-based motility.

We thank Mrs. M. Schmittner for skillful photographic assistance and Mrs. E. Eppacher for typing. We also thank Dr. M. Gimona and Kurt Anderson for comments on the manuscript, Prof. G. Oster for useful discussion, and Kurt Anderson and Klemens Rottner for moral support and help with the video microscopy. J.V. Small acknowledges the kind donation of *Listeria* by Prof. P. Cossart during the initial phase of this project.

The light microscope and imaging facility used for this work was purchased from funds granted by the Austrian National Bank and the Seegen Stifung of the Austrian Academy of Sciences, which are gratefully acknowledged.

Received for publication 3 December 1996 and in revised form 24 January 1997.

References

Anderson, K.I., Y.-L. Wang, and J.V. Small. 1996. Coordination of protrusion and translocation of the keratocyte involves rolling of the cell body. *J. Cell Biol.* 134:1209–1218.

Brundage, R.A., G.A. Smith, A. Camilli, J.A. Theriot, and D.A. Portnoy. 1993. Expression and phosphorylation of the Listeria monocytogenes ActA protein in mammalian cells. *Proc. Natl. Acad. Sci. USA.* 90:11890–11894.

Cudmore, S., I. Reckman, G. Griffiths, and M. Way. 1996. Vaccinia virus: a model system for actin-membrane interactions. *J. Cell Sci.* 109:1739–1747.

Dabiri, G.A., J.M. Sanger, D.A. Portnoy, and F.S. Southwick. 1990. Listeria monocytogenes moves rapidly through the host-cell cytoplasm by inducing directional actin assembly. *Proc. Natl. Acad. Sci. USA.* 87:6068–6072.

Dold, F.G., J.M. Sanger, and J.W. Sanger. 1994. Intact alpha-actinin molecules are needed for both the assembly of actin into the tails and the locomotion of Listeria monocytogenes inside infected cells. *Cell Motil. Cytoskeleton.* 28:97–107.

Domann, E., J. Wehland, M. Rohde, S. Pistor, M. Hartl, W. Goebel, M. Leimeister-Wächter, M. Wuenscher, and T. Chakraborty. 1992. A novel bacte-

rium virulence gene in Listeria monocytogenes required for host cell microfilament interaction with homology to the proline-rich region of vinculin. *EMBO (Eur. Mol. Biol. Organ.) J.* 11:1981–1990.
Franck, Z., R. Gary, and A. Bretscher. 1993. Moesin, like ezrin, colocalizes with actin in the cortical cytoskeleton in cultured cells, but its expression is more variable. *J. Cell Sci.* 105:219–231.
Heinzen, R.A., S.F. Hayes, M.G. Peacock, and T. Hackstadt. 1993. Directional actin polymerization associated with spotted fever group rickettsia infection of Vero cells. *Infect. Immun.* 61:1926–1935.
Herzog, M., A. Draeger, E. Ehler, and J.V. Small. 1994. Immunofluorescence microscopy of the cytoskeleton: Double and triple immunofluorescence. *In* Cell Biology: A Laboratory Handbook. J.E. Celis, editor. Academic Press, San Diego. 355–360.
Ishikawa, H., R. Bischoff, and H. Holtzer. 1969. Formation of arrowhead complexes with heavy meromyosin in a variety of cell types. *J. Cell Biol.* 43:312–328.
Kocks, C., E. Gouin, M. Tabouret, P. Merche, H. Ohayon, and P. Cossart. 1992. L. monocytogenes-induced actin assembly requires the actA gene product, a surface protein. *Cell.* 68:521–531.
Kocks, C., J.-B. Marchand, E. Gouin, H. D'Hautville, P.J. Sansonetti, M.-F. Carlier, and P. Cossart. 1995. The unrelated surface proteins ActA of *Listeria monocytogenes* and IcsA of *Shigella flexneri* are sufficient to confer actin-based motility on *Listeria innocua* and *Escherichia coli*, respectively. *Mol. Microbiol.* 18:413–423.
Lasa, I., and P. Cossart. 1996. Actin-based bacterial motility: towards a definition of the minimal requirements. *Trends Cell Biol.* 6:109–114.
Maupin-Szamier, P., and T.D. Pollard. 1978. Actin filament destruction by osmium tetroxide. *J. Cell Biol.* 77:837–852.
McKenna, N.M., and Y.-L. Wang. 1989. Culturing cells on the microscope stage. *Methods Cell Biol.* 29:295–305.
Mogilner, A., and G. Oster. 1996. Cell motility driven by actin polymerization. *Biophys. J.* 71:3501–3510.
Nanavati, D., F.T. Ashton, J.M. Sanger, and J.W. Sanger. 1994. Dynamics of actin and alpha-actinin in the tails of Listeria monocytogenes in infected PtK2 cells. *Cell Motil. Cytoskeleton.* 28:346–358.
Pollard, T.D. 1995. Missing link for intracellular bacterial motility? *Curr. Biol.* 5:837–840.
Sanger, J.M., J.W. Sanger, and F.S. Southwick. 1992. Host cell actin assembly is necessary and likely to provide the propulsive force for intracellular movement of Listeria monocytogenes. *Infect. Immun.* 60:3609–3619.
Sechi, A., and J.V. Small. 1997. Isolation of the actin comet tails of Listeria monocytogenes. *In* Cell Biology: A Laboratory Handbook II. J.E. Celis, editor. Academic Press, San Diego. In press.
Small, J.V. 1981. Organization of actin in the leading edge of cultured cells: influence of osmium tetroxide and dehydration on the ultrastructure of actin meshworks. *J. Cell Biol.* 91:695–705.
Small, J.V. 1985. Factors affecting the integrity of actin meshworks in cultured cells. *In* Cell Motility II. *Proc. Yamada Conf. on Cell Motility.* H. Ishikawa, S. Hatano, and H. Sato, editors. Nagoya, 1985. 493–506.
Small, J.V. 1988. The actin cytoskeleton. *Electron Microsc. Rev.* 1:155–174.
Small, J.V., and M. Herzog. 1994. Whole mount electron microscopy of the cytoskeleton: negative staining methods. *In* Cell Biology: A Laboratory Handbook. J.E. Celis, editor. Academic Press, San Diego. 135–139.
Smith, G.A., D.A. Portnoy, and J.A. Theriot. 1995. Asymmetric distribution of the Listeria monocytogenes ActA protein is required and sufficient to direct actin-based motility. *Mol. Microbiol.* 17:945–951.
Southwick, F.S., and D.L. Purich. 1996. Intracellular pathogenesis of Listeriosis. *N. Engl. J. Med.* 334:770–776.
Theriot, J.A. 1995. The cell biology of infection by intracellular bacterial pathogens. *Annu. Rev. Cell Dev. Biol.* 11:213–239.
Theriot, J.A., and T.J. Mitchison. 1991. Actin microfilament dynamics in locomoting cells. *Nature (Lond.).* 352:126–131.
Theriot, J.A., T.J. Mitchison, L.G. Tilney, and D.A. Portnoy. 1992. The rate of actin-based motility of intracellular Listeria monocytogenes equals the rate of actin polymerization. *Nature (Lond.).* 357:257–260.
Theriot, J.A., J. Rosenblatt, D.A. Portnoy, P.J. Goldschmidt-Clermont, and T.J. Mitchison. 1994. Involvement of profilin in the actin-based motility of Listeria monocytogenes in cells and cell-free extracts. *Cell.* 76:505–517.
Tilney, G.T., and D.A. Portnoy. 1989. Actin filaments and the growth, movement, and spread of the intracellular bacterial parasite, *Listeria monocytogenes. J. Cell Biol.* 109:1597–1608.
Tilney, L.G., and M.S. Tilney. 1993. The wily ways of a parasite: induction of actin assembly by Listeria. *Trends Microbiol.* 1:25–31.
Tilney, L.G., D.J. DeRosier, and M.S. Tilney. 1992*a.* How *Listeria* exploits host cell actin to form its own cytoskeleton. I. Formation of a tail and how that tail might be involved in movement. *J. Cell Biol.* 118:71–81.
Tilney, L.G., D.J. DeRosier, A. Weber, and M.S. Tilney. 1992*b.* How *Listeria* exploits host cell actin to form its own cytoskeleton. II. Nucleation, actin filament polarity, filament assembly, and evidence for a pointed end capper. *J. Cell Biol.* 118:83–93.
Zeile, W.L., D.L. Purich, and F.S. Southwick. 1996. Recognition of two classes of oligoproline sequences in profilin-mediated acceleration of actin-based *Shigella* motility. *J. Cell Biol.* 133:49–59.
Zhukarev, V., F. Ashton, J.M. Sanger, J.W. Sanger, and H. Shuman. 1995. Organization and structure of actin filament bundles in Listeria-infected cells. *Cell Motil. Cytoskeleton.* 30:229–246.